

## Article

# Antifrictional Effects of Group IVB Elements Deposited as Nanolayers on Anodic Coatings

Tadas Matijošius \* , Giedrius Stalnionis, Gedvidas Bikulčius, Sigitas Jankauskas, Laurynas Staišiūnas  and Svajus Joseph Asadauskas 

State Research Institute Center for Physical Sciences & Technology (FTMC),  
Sauletekio 3, LT 10257 Vilnius, Lithuania

\* Correspondence: tadas.matijosius@ftmc.lt; Tel.: +370-5-264-9210

**Abstract:** The utilization of anodized aluminum (Al) components would contribute greatly to combat against dry friction if good tribological properties could be attained. Despite its hardness, the wear rate of anodic coatings presents a major problem in many applications, including automotive, aerospace and high-tech industries. Recently, nanolayers of Ti demonstrated high tribological effectiveness and unusually low dry friction on anodic coatings. However, few researchers focus on the tribological characterization of nanolayers of other elements. In this study, nanolayers of Ti, Zr, Hf, Cu, Cr, Nb and Sn were deposited on anodized 1050 and 6082 alloys by magnetron sputtering and Atomic Layer Deposition. Major attention was devoted to surface roughness and hardness measurements, because of their importance for static friction. The results showed that structural, chemical and other intrinsic properties of nanolayers of Group IVB elements in many cases led to significant friction reduction, when compared to those of Cu, Cr and Hf. Nanolayers of 15 nm to 75 nm thicknesses appeared most effective tribologically, while 180 nm or thicker layers progressively lost their ability to sustain low dynamic friction. Deposition of nanoscale structures could provide advantages for the anodized Al industry in protection against incidental friction and wear.

**Keywords:** anodic alumina; nanolayers; static friction; hardness



**Citation:** Matijošius, T.; Stalnionis, G.; Bikulčius, G.; Jankauskas, S.; Staišiūnas, L.; Asadauskas, S.J. Antifrictional Effects of Group IVB Elements Deposited as Nanolayers on Anodic Coatings. *Coatings* **2023**, *13*, 132. <https://doi.org/10.3390/coatings13010132>

Academic Editor: Huirong Le

Received: 19 December 2022

Revised: 5 January 2023

Accepted: 8 January 2023

Published: 10 January 2023



**Copyright:** © 2023 by the authors. Licensee MDPI, Basel, Switzerland. This article is an open access article distributed under the terms and conditions of the Creative Commons Attribution (CC BY) license (<https://creativecommons.org/licenses/by/4.0/>).

## 1. Introduction

The deposition of polytetrafluoroethylene (PTFE), diamond-like carbon (DLC) coatings greatly benefit combat against dry friction, leading to less waste and simpler maintenance over liquid lubricants. Unfortunately, without a fundamental understanding, it is hard to explain why coatings, films and layers reduce friction. The reduction of surface friction and wear often depends on tribofilm formation. The adsorbed film is usually formed by intermolecular forces, while the tribofilm formation is influenced by tribochemical reactions and depends on structure, chemical composition and tribological behavior. In general, during dry friction tribofilm formation mostly form from wear debris [1]. They might have soft inclusions originating from multi-phase or composite coatings with graphite [2], WS<sub>2</sub> [3], MoS<sub>2</sub> [4], which can be transferred during sliding, leading to the formation of transfer tribofilm. MoS<sub>2</sub> and WS<sub>2</sub> have the best load-carrying capacity and low shear strength as thin solid layers, due to the anisotropic lamellar structure, covalent bonding within the adjacent lamellae and weak Van der Waals forces between them. DLC coatings may produce tribofilm formation dependent on the phase transformation of the surface. The sliding-induced transformation from sp<sup>3</sup> diamond structure to sp<sup>2</sup> graphite structure reduces the Coefficient of Friction (COF) from 0.20 to 0.05 [5]. Some tribofilms are generated due to tribochemical reactions between the wear debris and oxygen or moisture [6].

Since engineering surfaces are usually exposed to oxygen, it would be reasonable to study the most fundamental aspects of interactions in the friction zone of oxide layers. Metal oxide nanoparticles, including ZnO, CuO and a few others, could be used as lubricant

additives for friction reduction [7]. Low friction and anti-wear properties are related to the deposition of nanoparticles in the friction zone and the rolling effect, which can reduce shearing stress and improve tribological properties. Nevertheless, metal oxides are rarely used for dry friction on hard substrates because of high melting points, poor elasticity and response to shear. Some metal oxides, such as  $\text{Al}_2\text{O}_3$ , might even demonstrate highly abrasive properties. Therefore, the tribological behavior of nanolayers of Ti and its oxides reducing COF below 0.2 on porous alumina substrates under dry friction conditions [8,9] appears to be quite unusual. The thickness of the layer is very important because thick Ti oxides often provide lower COF, as demonstrated by thermally oxidized Ti coating with COF of  $\sim 0.35$  [10] and plasma-sprayed  $\text{Al}_2\text{O}_3/\text{TiO}_2$  composite with COF  $\sim 0.5$  on steel substrate [11]. The importance of surface roughness and other topographical properties on friction reduction cannot be excluded either. The textural patterns might act as reservoirs, able to entrap and release lubricants in the friction zone [12], which is beneficial for static friction during the “running-in” friction stages.

The advancement of hard coatings with high friction and wear resistance find consideration in biomedical, robotic and other high-tech applications. For example, thermally oxidized Zr possesses higher hardness and two times higher scratch resistance when compared to thermally oxidized Ti [13]. In the case of hard chromium (Cr) coatings, trivalent Cr plating is considered a very promising technology to replace hazardous hexavalent Cr due to its high corrosion and wear resistance [14]. On the other hand, the deposition of soft metals on hard substrates is an alternative way to improve tribological properties. In the case of Cu, Sn, Pb, Ag and several other metals the so-called servovitic effect might be achieved, as demonstrated on steel and bronze alloys [15,16]. Evaluation of static friction and the early stages of friction might provide more information on fundamental aspects of tribology.

In this study, nanolayers of group IVB (Ti, Zr, Hf) elements and several additional metals, including Cr, Cu and Nb, were deposited on anodic coatings of industrially relevant Al alloys 1050 and 6082 in order to combat dry friction losses. While a significant portion of the data was retrieved from previous publications [17,18], new microscopy images, roughness measurements and conceptual interpretations are also provided. A preliminary assessment of the thin Sn layers is also presented. Major attention was devoted to surface roughness and hardness measurements, which have a high influence on static friction.

## 2. Materials and Methods

Al alloys 1050 of 99.67% purity (0.25% Fe; 0.08% Si) and 6082 of 96.72% (1.10% Si; 1.02% Mg; 0.61% Mn; 0.54% Fe), with a sheet thickness of 2 mm, from FXB-Niemet UAB (Lithuania), were used as substrates for anodization and deposition of group IVB and other metals as nanolayers on anodic coatings. Most of the equipment and procedures, including hard anodizing, microscopy and tribotesting had already been presented previously [9,17,18]. Briefly, their descriptions are provided below.

### 2.1. Hard Anodization

Hard (Type III) anodization was performed in  $\text{H}_2\text{SO}_4$ /oxalic acid electrolyte to produce relatively thick  $\text{Al}_2\text{O}_3$  coatings of 50 to 60  $\mu\text{m}$  thickness, as described previously [18]. For optimal anodization conditions, current density was set at 2  $\text{A}/\text{dm}^2$ , electrolyte temperature at 15  $^\circ\text{C}$  and an anodization time of 70 min was retained. After anodization, the specimens were rinsed in a bath of deionized (DI) at room temperature. Then the specimens were dried at 50  $^\circ\text{C}$  for 60 min before deposition and tribotesting.

### 2.2. Deposition of Nanolayers

The deposition of monometallic group IVB (Ti, Zr, Hf) and additional Cr, Cu and Nb elements as nanolayers was performed on anodic coatings by means of a DC/RF magnetron sputtering device Univex 350 (Leybold Vacuum Systems, Köln, Germany). Before sputtering, the chamber was evacuated at 250  $\mu\text{Pa}$  and the working pressure of

Ar gas was kept constant at 250 mPa, maintaining substrate temperature at 12 °C. The target thickness of nanolayers was obtained by changing sputtering parameters including time, current and voltage [19]. The targets were pre-etched using Ar<sup>+</sup> ion beams for 10 min at 100 W before sputtering to remove surface oxides, nitrides and other contaminants. Sputtering duration, current and voltage were adapted to achieve 16 nm and 75 nm thicknesses, respectively [19]. The rotary sample holder was turned during the sputtering at 20 rpm to ensure uniform patterns of the deposited layers.

The formation of TiO<sub>2</sub> and HfO<sub>2</sub> nanolayers was performed by Atomic Layer Deposition (ALD). The nanolayers were deposited by the Fiji F200 system (Cambridge NanoTech Inc., Cambridge, MA, USA) at 250 °C and 30–35 Pa vacuum [9]. Tetrakis(dimethylamino) titanium (TDMAT) and tetrakis(dimethylamino) hafnium (TDMAH) precursors from Strem Chemicals of 99% purity were used for TiO<sub>2</sub> and HfO<sub>2</sub> respectively. The 375 cycles for TiO<sub>2</sub> and 158 cycles for HfO<sub>2</sub> resulted in 15 nm thickness.

Cross-sectional analysis involved measuring the layer thickness by cutting cross sections of nanostructured coatings or making use of X-ray photoelectron spectroscopy (XPS) to determine the thickness of Ti and its oxides, as demonstrated previously [8,9]. In this study, to obtain the thickness of nanolayers grazing XRD was first attempted but the results were inconclusive, so, instead of directly measuring on anodic coatings, the deposition rates of nanolayers were established by means of X-ray reflectivity (XRR) on a SmartLab diffractometer (Rigaku, Tokyo, Japan), using an indirect method on polished silicon or glass substrates [20].

### 2.3. Tribotesting

A Pin-on-Disc Tribometer from Anton Paar (Buchs, Switzerland) was used for friction tests. A corundum ball of 6 mm outer diameter (OD) and 99.8% purity, from RGP International Srl (Balsamo, Italy), was held stationary. The specimen was mounted on a tribometer module and maintained a linear reciprocal configuration of 2 mm amplitude, 2 cm/s velocity and 10 N load for a maximum of 1000 friction cycles, resulting in one full friction cycle being 8 mm. At 2 cm/s for each friction cycle a 100 data points per second rate was applied for greater sensitivity in measuring ‘instantaneous’ frictional force, the values of which remained similar and in the 80% segment, through the selected reciprocal motion range. In the segment, the line of COF=0 was established with equal areas of ‘negative’ and ‘positive’ areas under the peaks.

The duration of the tribotest was either automatically limited, due to excessive frictional force because of an increase in COF, or stopped after a specified number of friction cycles. Static COF, representing the highest friction force of the first friction cycle required to start sliding motion, was measured as described previously [17].

### 2.4. Microscopy and Roughness Measurements

Scanning Electron Microscopy (SEM) employed images were obtained using Helios NanoLab 650 (FEI, Hillsboro, OR, USA). Thin layers of Cr were applied at 2–3 nm thickness to all specimens in order to obtain the necessary electrical conductivity with the magnetron sputtering device Quorum Q150T ES (Judges Scientific Plc, London, UK). An Energy-Dispersive X-ray (EDS) spectrometer, INCA Energy 350 X-Max 20 EDS, was employed for elemental analysis, using an INCA spectrometer with an X-Max 20 mm<sup>2</sup> Silicon-drift detector (Oxford Instruments, Abingdon, UK) to examine the morphology and composition of the nanostructured coatings at 20 kV accelerating voltage. Beforehand, thin layers of Cr were applied at 2–3 nm thickness to ensure the necessary electrical conductivity with a magnetron sputtering device, Quorum Q150T ES (Judges Scientific Plc). The elemental composition was reported as atomic weight percentage, using an accelerating voltage of 20 kV.

A stylus profilometer, SurfTest SJ-210 (Mitutoyo, Aurora, IL, USA) scanned the surfaces horizontally, with a path length of 1.5 mm, at least five times at random locations, with a diamond tipped needle of 2 µm radius, to evaluate the following surface roughness

parameters: arithmetic mean ( $Ra$ ), root mean squared ( $Rq$ ), maximum peak height above the mean line ( $Rp$ ), maximum valley depth below the mean line ( $Rv$ ), maximum peak to valley height ( $Rz$ ), skewness ( $Rsk$ ) and kurtosis ( $Rku$ ).

### 2.5. Hardness by Indentation

Indentation tests were performed on anodic coatings sputtered with Ti layers. The Hysitron Ti Premier system, having a high load transducer (Bruker, Billerica, MA, USA), equipped with a Berkovich diamond indenter, with an angle of  $142.3^\circ$ , was used for the indentations. The tip was calibrated on a fused quartz surface, with a hardness of 9.25 GPa and a reduced modulus of 69.6 GPa.

Single indentations were made, in the range of 4 mN to 3 N, with loading and unloading times set to 2 s and load hold time set to 1 s, respectively. The depth scan was performed in a series of 50 load hold, partial unload, cycles at 2 s, 1 s, 2 s intervals, increasing the penetration depth up to 5  $\mu\text{m}$  [18]. The data from several hundreds of nanometers were marked as surface segment data (100–200 nm in depth), and data from 2 to 3  $\mu\text{m}$  of depth as substrate segment. Hardness data were registered in GPa. The maximum loading force never exceeded 3 N during the depth scan. The final hardness values were calculated using TriboScan software, version 9.

## 3. Results and Discussion

Metals and their oxides of group IVB elements along with other metals, including Cr, Cu, Nb and Sn, were deposited as nanolayers on anodic coatings. The latter four metals are recognized for having tribological effectiveness. Two distinctly different Al alloys, 1050 and 6082, were selected for surface nanostructuring and tribological experiments.

### 3.1. Characterization of Nanolayers of IVB Metals

Industrial alloys 1050 and 6082 were used for anodization to produce porous  $\text{Al}_2\text{O}_3$  coatings of 50–60  $\mu\text{m}$  thickness, with an average nanopore inside diameter (ID) of 7 nm and 15 nm for 1050 and 6082, respectively. Nanolayers of Ti, Zr and Hf and their oxides of similar thicknesses were deposited by magnetron sputtering and ALD. For better data segregation, nanolayers of 15 nm thickness were attributed to ALD, whereas nanolayers of 16 nm thickness were attributed to magnetron sputtering. It was reasonable to investigate oxide layers, since thin films of many metals undergo significant oxidation quite rapidly in an ambient environment.

Surface nanotopography revealed that the deposition of 15–16 nm layers was sufficient to fully cover the openings of the nanopores of anodic coatings, as noted in the previous report [18], Figure 1. The differences in microscale patterns had already been noted on both anodized Al alloys, possibly due to grain boundaries. However, it is more probable that these net-like structures were the result of the anodic coating formation, rather than the nanolayer deposition. The coating formation process was not totally uniform and some coating segments grew faster than others, resulting in an uneven surface, even at the nano-scale. After depositing the nanolayers, the edges of these segments produced insulating effects, which led to bright bands in SEM images, due to reflected electrons. However, at lower magnification, the surfaces appeared quite similar, without significant agglomerations or discontinuities in general. From a tribological standpoint, microscale and macroscale patterns are very important, because cracking, waviness, bulging and other imperfections strongly affect friction trends and wear propagation. Interestingly, the surfaces appeared relatively uniform and homogeneous on nanostructured 1050 at the nanoscale level. Net-like structures became even more visible after deposition on the 6082 alloy. This indicated that the homogeneity of nanostructured 6082 alloys was poorer at the nanoscale level.

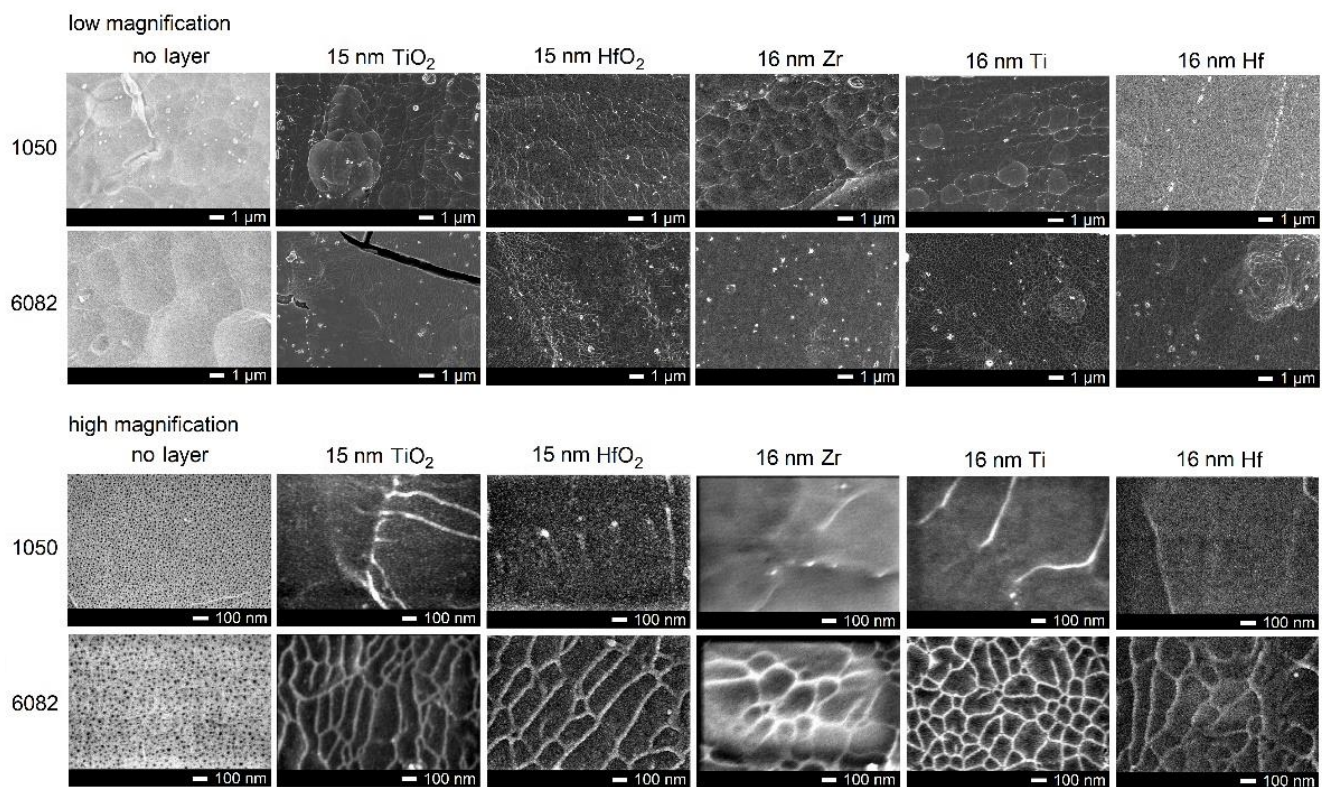


**Figure 1.** SEM images of anodic coatings with nanolayers of group IVB transition metals, deposited by ALD (15 nm) or sputtering (16 nm) under low (**top**) and high (**bottom**) magnifications. The high magnification images were adapted with permission from [18], 2021, Elsevier.

According to the EDS elemental analysis, ALD specimens showed a higher abundance of deposited elements, rather than sputtered specimens, especially for Ti/TiO<sub>2</sub> layers, as demonstrated in Table 1 [19].

**Table 1.** EDS analysis of deposited nanolayers of group IVB elements on anodic coatings, adapted from [19].

Deposition and Layer Thickness, nm	Alloy	Elemental Composition, at. %				
		Al	O	Hf/Ti/Zr	Si	S
no layer	1050	26.89	69.33	0	0	3.78
0 nm	6082	32.13	63.40	0	0.41	4.06
Hf (sputtering)	1050	32.42	62.64	0.90	0	4.04
16 nm	6082	31.66	62.92	0.96	0.63	3.84
HfO <sub>2</sub> (ALD)	1050	32.57	62.59	0.94	0	3.89
15 nm	6082	32.10	63.37	0.85	n.d.	3.68
TiO <sub>2</sub> (ALD)	1050	31.93	62.53	1.41	0.05	4.08
15 nm	6082	31.61	62.17	1.97	0.34	3.91
Ti (sputtering)	1050	31.51	64.66	0.35	0	3.47
16 nm	6082	31.09	64.39	0.38	0.38	3.77
Zr (sputtering)	1050	30.06	66.00	0.16	0	3.78
16 nm	6082	29.26	66.54	0.17	0.33	3.70

The penetration of TiO<sub>2</sub> into the anodic coating by ALD was deeper than that of sputtered Ti. Moreover, anodic coatings on 6082 alloys, whose nanopores were twice as wide, were able to accumulate a higher abundance of deposited elements. It was reasonable to expect that the anodic coating of 6082 alloys would have higher surface roughness *Ra* values than those of 1050 due to lower homogeneity, i.e.,  $1.28 \pm 0.08 \mu\text{m}$  vs.  $0.86 \pm 0.09 \mu\text{m}$ . Several roughness parameters, including *Ra*, *Rp*, *Rv*, *Rsk*, reported

in [18], and the additional parameters of  $Rq$ ,  $Rz$ ,  $Rku$ , were selected to assess the surface roughness of anodized 6082 alloys sputtered with 16 nm, 75 nm, 185 nm and 515 nm Ti layers. However, the deposition of 75 nm nanolayers and thicker Ti layers did not produce a statistically significant change in roughness parameters, except for  $Rz$  and  $Rp$ , it still provided valuable information about surface topography, see Figure 2.

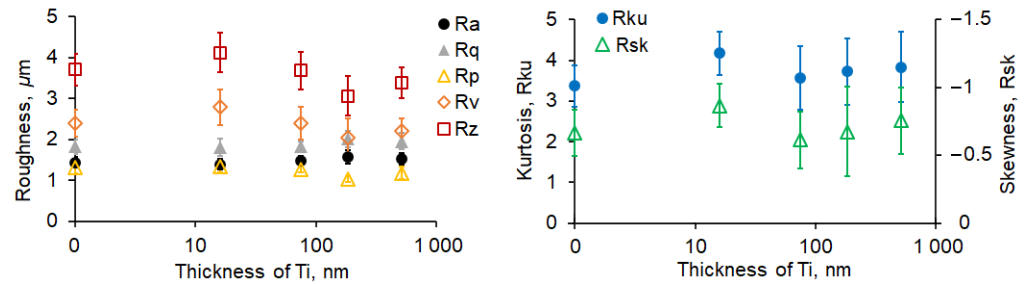


Figure 2. Influence of sputtered Ti layer thickness on surface roughness of hard anodized 6082 alloys.

Thicker Ti layers covered the nanopores of anodic coatings and were able to reduce the depth of valleys. Some drop in  $Rz$  and  $Rp$  values could be noted for the layers of 185 nm thickness, although this effect was not very statistically significant. This might be explained as due to more Ti accumulating in the valleys, but the error bars of  $Rz$  and  $Rp$  for 185 nm thickness nearly overlapped with those at 16 nm thickness, so such substantiation was not very convincing. A negative value of  $Rsk$  indicated that all surfaces were made up of valleys, rather than peaks or asperities. Negative skew was sometimes correlated with good tribological performance, e.g., in the case of bearing surface. The high depth of valleys and unevenness of the surface were also validated by  $Rv$  and  $Rz$  values, respectively. Another parameter,  $Rku$ , could be related to the sharpness of the profile peaks through their kurtosis. The statistical studies showed that the lowest value of  $Rsk$  and the highest value of  $Rku$  suggested the best tribological performance and lowest COF [21]. The Ti layer of 16 nm thickness, with the highest  $Rku$  and lowest  $Rsk$ , was also able to reduce friction. This was in agreement with other researchers [21], who suggested that a higher difference between kurtosis and skewness could benefit tribological performance.

Surface hardness is another important parameter that often affects friction trends. In this study, indentation hardness measurements were segregated into surface segment data (100 to 200 nm in depth) and substrate segment data (2–3 µm in depth), assuming a maximum depth value of 5 µm for indentation. Indentation hardness of the surface segment appeared to reduce with increasing thickness of Ti layers from 16 to 515 nm, as seen in Figure 3.

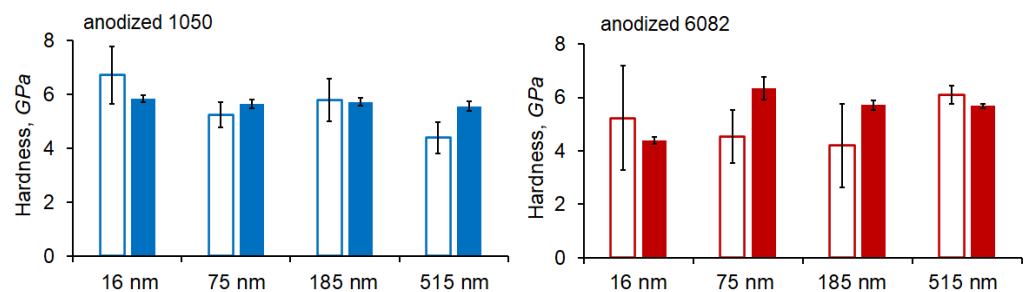


Figure 3. Influence of thickness of Ti layers on the indentation hardness of anodized 1050 and 6082 alloys. Depth-scan values for a surface segment (hollow bars: 100–200 nm) and substrate segment (solid bars: 2–3 µm).

The hardness values of sputtered Ti layers decreased slightly with higher thickness of the Ti layer on anodized 1050 when considering the surface segment data. The substrate segment data did not show any significant change. In the case of anodized 6082,

the error bars were much higher for the surface segment data, rendering these results inconclusive, which might be caused by higher surface roughness. The more evident trend of hardness reduction on 1050 might be related to its relatively hard anodic coating. As reported previously [18], the substrate hardness of anodized 1050 and 6082, before the deposition of nanolayers, were 6.6 GPa and 5.0 GPa, respectively. As the Ti layer might be somewhat softer, its effect was more obvious on anodized 1050. However, no correlation was evident between these values and the nature of group IVB elements or friction trends, in agreement with previous findings [18]. On the other hand, the measured values of indentation hardness of Ti layers were strongly affected by the hardness of the anodic coating itself, and should not be attributed to the actual hardness of the nanolayers due to instrumental limitations.

### 3.2. Friction of Nanolayers of IVB Metals

The friction of nanolayers of group IVB elements was tested using a chemically inert corundum ball of ~2900 Vickers Hardness (HV) to reduce the influence of counterbody-induced reactions. All friction tests showed very good repeatability [20], suggesting the formation of nanolayers with high uniformity. For a better understanding of the differences of group IVB elements for frictional reduction, static COF and dynamic COF values after 10 cycles were adapted from previous results [18]. The deposited nanolayers reduced static COF with an average value less than 0.2 on both anodized 1050 and 6082 alloys, which was significantly lower than the plain anodic coating with COF over 0.4, as seen in Figure 4.

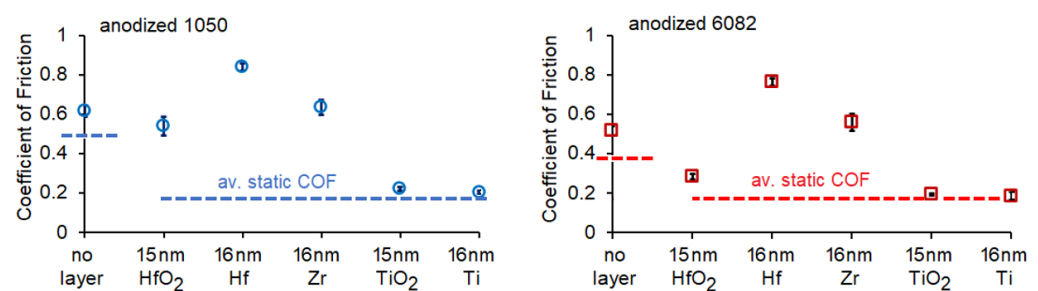


**Figure 4.** Influence of nanolayers of group IVB elements on friction after 10 cycles deposited on anodized 1050 (left) and 6082 (right) alloys, adapted with permission from [18]. 2021, Elsevier.

However, the antifrictional properties of nanolayers of IVB elements changed dramatically after 10 friction cycles. Only nanolayers of Ti and TiO<sub>2</sub> retained low COF ~0.2, while Zr, Hf and its oxides lost their tribological effectiveness. It was expected that the oxide layer could have a huge impact on friction reduction because the sputtered Ti nanolayer, the composition of which might be expected to be metallic, showed nearly full oxidation in an ambient environment, as demonstrated by XPS [9]. In the case of sputtered Zr and Hf, the oxidation to ZrO<sub>2</sub> and HfO<sub>2</sub>, respectively, had a much smaller effect on friction, compared to the oxidation of Ti into TiO<sub>2</sub>. The depletion of the oxide layer of IVB elements led to higher friction, wear debris formation in the friction zone and, eventually, to abrasion with high COF fluctuations and major wear increase at the latest frictional stages. The low static friction of deposited Ti/TiO<sub>2</sub> nanolayers depended on their intrinsic properties, rather than surface roughness, morphology or interaction with the substrate. It was unlikely that Ti or TiO<sub>2</sub> could react with chemically inert Al<sub>2</sub>O<sub>3</sub>. The relevance of surface roughness and hardness on friction reduction could probably be excluded, since the values of all related parameters of group IVB nanolayers were quite similar, due to relatively large error bars.

Magnetron sputtering was used to deposit Ti layers from 16 to 515 nm in thickness. While Ti layers of 15–75 nm thickness effectively reduced COF for at least 10 friction cycles, 180 nm or thicker layers did not reduce friction significantly and gradually the ability to maintain low COF was lost, Figure 5.

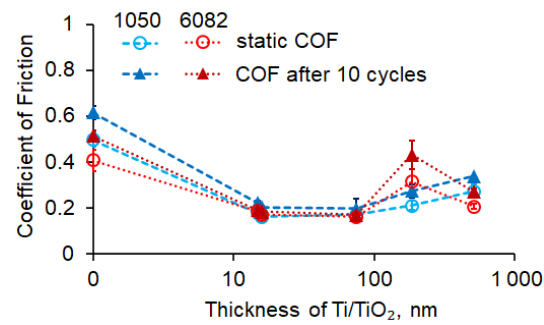


**Figure 5.** Influence of Ti layers thickness on static friction (hollow signs) and friction after 10 cycles (solid signs) on anodized 1050 and 6082 alloys.

Previous studies showed that Ti layers of 2.3  $\mu\text{m}$  thickness increased static COF to 0.4 for anodized 1050 and  $>0.5$  for anodized 6082 alloys, which were considered high [8]. Since oxidation was restricted during magnetron sputtering, the oxidation of submicron or micron scale Ti layers might not be as complete as for nanolayers. Such results support the idea that structural, chemical and other intrinsic properties of Ti nanolayers are the main drivers of tribological effectiveness. Some tribological mechanisms were explained recently using water-based lubricants, with  $\text{TiO}_2$  nanoparticles on ferritic stainless steel, by the formation of tribofilm with the ball-bearing effect [22]. However, these conclusions could not be supported, either by the tribological trends nor by SEM microscopy at lower magnification, Figure 1, which did not show any distinct ball-like aggregates.

### 3.3. Friction of Nanolayers of 75 nm and Higher Thickness

Several other Group B elements, including Cr, Cu and Nb, as well as Sn from Group IVA, were deposited on anodic coatings, due to their high hardness and possible servovitic effects for frictional reduction. Data were combined from previous reports [18,20] to show the antifrictional mechanisms based on Group B elements. The data showed that Hf and hard Cr layers increased COF much more, when compared to anodic coatings, after 10 friction cycles, with high reproducibility, as seen in Figure 6.

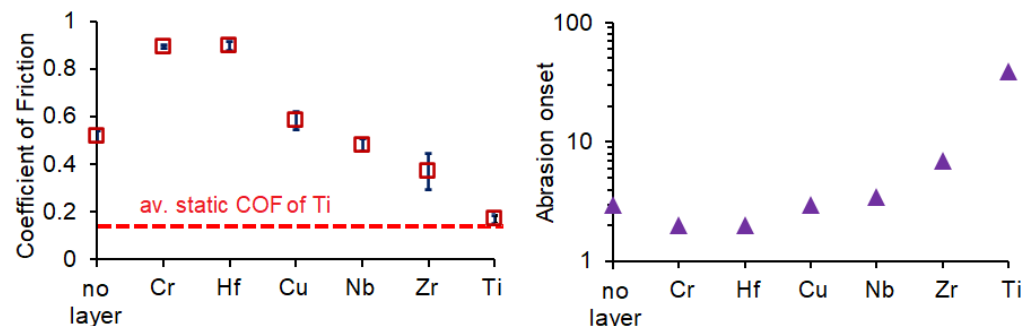


**Figure 6.** Influence of 75 nm layers on static friction after 10 cycles (left) and abrasion onset dynamic friction (right) on anodized 6082 alloy.

Higher friction was observed on anodized 6082 alloys, with sputtered Hf layers, especially regarding dynamic friction. In contrast, soft metals, like Cu, appeared to reduce friction by dissipating shear, or by forming servovitic films on hard substrates [15]. However, the thickness of the Cu nanolayer might be too low for these phenomena to take place as implied, due to having very similar tribological behavior to anodic coatings. The statistically lower surface parameter of  $R_{sk}$  and  $R_{ku}$  at 75 nm Cu layers suggested that these values were not significant for frictional reduction. Both Zr and Ti nanolayers provided the lowest static friction below 0.2, but only Ti suggested the best antifrictional properties, sustained up to 30 friction cycles until abrasion onset was observed. Although the abrasion onset of many nanolayers was not clearly detectable, the Zr and Ti layers displayed strongly

expressed thresholds, showing the beginning of severe abrasion. The high reproducibility of dynamic friction for the 75 nm layers meant error bars were insignificant. The Zr layers also showed promising trends in frictional reduction, but were less effective than Ti.

In previous reports, some effort was devoted to establishing the mechanism for the antifrictional effect of Ti nanolayers [8,18]. In many cases, COF rose gradually with progressing friction beyond some initial delay. As a possible explanation of such a tendency, ball-like aggregates, or servovitic effects, were suggested, but their contributions were considered insignificant [18]. Since a high concentration gradient of Ti in the frictional zone was observed by detecting the variation of %Ti from 0.77 wt.% to 8.73 wt.% within less than 30  $\mu\text{m}$  on the wear track [8], a more likely explanation would be a quasi-fluid behavior of the Ti nanolayers. Such fluidity of the Ti nanolayer in the frictional zone should not be confused with the action of Anti Wear additives or similar tribofilms in liquid lubricants [23]. Quasi-fluid behavior is more closely affiliated to the wear mechanisms in thin films or layers of wear debris. In any case, such quasi-fluid behavior might help to distribute the interfacial pressure more evenly between the asperities [24], thus reducing highly localized stresses and improving tribological performance.

The layers of Cr, Nb, and Zr, and possibly Ti, of 75 nm thicknesses were somewhat harder than the anodic coating. However, the influence of hardness on frictional tendencies was not an important factor, since Ti and Zr layers show completely different tendencies when compared to hard Cr.

As presented in Figure 5, the higher thickness of Ti layer not only did not provide any improvement in COF but actually increased dynamic friction. While other tested elements were screened at 75 nm nanolayer thickness, Sn was deposited at 375 nm thickness and its friction trends compared to those of Ti of neighboring thickness, are seen in Figure 7.

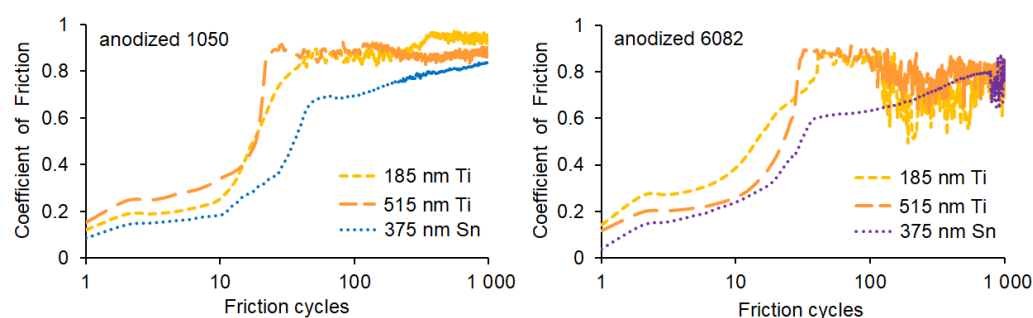


**Figure 7.** Comparison of friction trends of Sn and Ti layers sputtered on anodic coatings of 1050 (**left**) and 6082 (**right**) alloys at 185–515 nm thickness.

Apparently, a thin Sn layer might achieve a somewhat better tribological performance than that of Ti when the thickness was around 300–400 nm or so. Such layer thickness was less tribologically favorable for Ti, compared to its 15–75 nm nanolayers. Nevertheless, the retention of low COF appeared better for these Sn layers and was significantly better than those of other elements tested in this study. Therefore, further attention should be devoted to nano-thin layers of Sn and to possible improvements in their tribological performance. It is too early to forecast the opportunities for tin nanolayers, but intrinsic properties of nanolayers of IVB elements suggest new applications of anodized Al in the high-tech industry, biomedicine, aerospace and other areas. More detailed investigations of tribological tendencies, along with hydrolysis of nanolayers and surface oxidation under a humid atmosphere, might provide more information about the mechanisms related to low friction.

#### 4. Conclusions

Nanolayers of Group IVB and several other group B elements were successfully deposited on anodic coatings using ALD and sputtering. The layers were characterized by SEM, EDS and indentation. A Pin-on-Disc tribometer was used for tribological measure-

ments using a chemically inert corundum ball and 10 N load. The layer thickness was 75 nm in most cases, but 15 nm and 515 nm were also tested for Ti layers, as well as 375 nm for Sn layers. Several conclusions could be drawn, as follow:

1. Nanolayers of Ti and its oxides are tribologically more effective on anodic coatings than other IVB elements. At 180 nm or higher thickness, Ti layers progressively lose their ability to sustain low friction.
2. Tin layers of 375 nm demonstrate better tribological performance than Ti of similar thickness.
3. Nanolayers of HfO<sub>2</sub> and Zr show effectiveness in static COF reduction.
4. Nanolayers of Cr, Cu and Nb do not show frictional reduction on anodic coatings.
5. Although the parameters of nanolayer hardness and roughness did not show a statistically valid correlation to the friction tendencies, the higher difference between kurtosis and skewness matched the instance of low friction in several cases.

**Author Contributions:** Conceptualization, S.J.A.; methodology, T.M., G.B., S.J., L.S. and S.J.A.; validation, T.M., G.B. and L.S.; formal analysis, T.M.; investigation, T.M., G.S., G.B. and L.S.; resources, S.J.A.; writing—original draft preparation, T.M.; writing—review and editing, S.J.A.; visualization, T.M. and S.J.A.; supervision, S.J.A. All authors have read and agreed to the published version of the manuscript.

**Funding:** This research was funded by Lithuanian federal research, grant number 01.2.2-CPVA-K-703-03-0024.

**Institutional Review Board Statement:** Not applicable.

**Informed Consent Statement:** Not applicable.

**Data Availability Statement:** The raw data required to reproduce these findings are available to download from [<https://doi.org/10.5281/zenodo.5517525> (accessed on 3 January 2023)]. The processed data required to reproduce these findings are available to download from [<https://doi.org/10.5281/zenodo.5517525> (accessed on 3 January 2023)].

**Acknowledgments:** The authors acknowledge the activity under Measure 09.3.3-LMT-K-712 ‘Development of Scientific Competences of Scientists, other Researchers and Students through Practical Research Activities’ (Funding instrument—European Social Fund). The implementation of the measure is managed by the Ministry of Education, Science and Sport of the Republic of Lithuania and the Research Council of Lithuania.

**Conflicts of Interest:** The authors declare no conflict of interest.

## References

1. Luo, Q. Origin of friction in running-in sliding wear of nitride coatings. *Tribol. Lett.* **2010**, *37*, 529–539. [[CrossRef](#)]
2. Sun, W.C.; Zhang, P.; Zhao, K.; Tian, M.M.; Wang, Y. Effect of graphite concentration on the friction and wear of Ni–Al<sub>2</sub>O<sub>3</sub>/graphite composite coatings by a combination of electrophoresis and electrodeposition. *Wear* **2015**, *342–343*, 172–180. [[CrossRef](#)]
3. Gustavsson, F.; Svahn, F.; Bexell, U.; Jacobson, S. Nanoparticle based and sputtered WS<sub>2</sub> low-friction coatings—Differences and similarities with respect to friction mechanisms and tribofilm formation. *Surf. Coat. Technol.* **2013**, *232*, 616–626. [[CrossRef](#)]
4. Sahoo, R.R.; Biswas, S.K. Microtribology and friction-induced material transfer in layered MoS<sub>2</sub> nanoparticles sprayed on a steel surface. *Tribol. Lett.* **2010**, *37*, 313–326. [[CrossRef](#)]
5. Ronkainen, H.; Holmberg, K. Environmental and thermal effects on the tribological performance of DLC coatings. In *Tribology of Diamond-Like Carbon Films*; Donnet, C., Erdemir, A., Eds.; Springer: Boston, MA, USA, 2008; pp. 155–200.
6. Liew, W.Y.H. Effect of relative humidity on the unlubricated wear of metals. *Wear* **2006**, *260*, 720–727. [[CrossRef](#)]
7. Uflyand, I.E.; Zhinzhiro, V.A.; Burlakova, V.E. Metal-containing nanomaterials as lubricant additives: State-of-the-art and future development. *Friction* **2019**, *7*, 93–116. [[CrossRef](#)]
8. Matijošius, T.; Ručinskienė, A.; Selskis, A.; Stalnionis, G.; Leinartas, K.; Asadauskas, S.J. Friction reduction by nanothin titanium layers on anodized alumina. *Surf. Coat. Technol.* **2016**, *307*, 610–621. [[CrossRef](#)]
9. Matijošius, T.; Pivoriūnas, A.; Čebatariūnienė, A.; Tunaitis, V.; Staišiūnas, L.; Stalnionis, G.; Ručinskienė, A.; Asadauskas, S.J. Friction reduction using Nanothin Titanium layers on anodized aluminum as potential bioceramic material. *Ceram. Int.* **2020**, *46*, 15581–15593. [[CrossRef](#)]
10. Krishna, D.S.R.; Brama, Y.L.; Sun, Y. Thick rutile layer on titanium for tribological applications. *Tribol. Int.* **2007**, *40*, 329–334. [[CrossRef](#)]

11. Dejang, N.; Watcharapasorn, A.; Wirojupatump, S.; Niranatlumpong, P.; Jiansirisomboon, S. Fabrication and properties of plasma-sprayed Al<sub>2</sub>O<sub>3</sub>/TiO<sub>2</sub> composite coatings: A role of nano-sized TiO<sub>2</sub> addition. *Surf. Coat. Technol.* **2010**, *204*, 1651–1657. [[CrossRef](#)]
12. Guleryuz, C.G.; Krzanowski, J.E. Mechanisms of self-lubrication in patterned TiN coatings containing solid lubricant microreservoirs. *Surf. Coat. Technol.* **2010**, *204*, 2392–2399. [[CrossRef](#)]
13. Alansari, A.; Sun, Y. A comparative study of the mechanical behaviour of thermally oxidised commercially pure titanium and zirconium. *J. Mech. Behav. Biomed. Mater.* **2017**, *74*, 221–231. [[CrossRef](#)] [[PubMed](#)]
14. Bikulcius, G.; Češunienė, A.; Selskienė, A.; Pakštas, V.; Matijošius, T. Dry sliding tribological behavior of Cr coatings electrodeposited in trivalent chromium sulphate baths. *Surf. Coat. Technol.* **2017**, *315*, 130–138. [[CrossRef](#)]
15. Garkunov, D.N. Self-organizing processes in tribological system under friction interaction. In *Handbook on Tribology*; Hebda, M., Chichnadze, A.V., Eds.; Machinostroenie: Moscow, Russia, 1989; p. 288.
16. Burlakova, V.E.; Milov, A.A.; Drogan, E.G.; Novikova, A.A. Nanotribology of Aqueous Solutions of Monobasic Carboxylic Acids in a Copper Alloy—Steel Tribological Assembly. *J. Surf. Invest-X-Ray* **2018**, *12*, 1108–1116. [[CrossRef](#)]
17. Matijošius, T.; Gedvilas, M.; Gečys, P.; Vozgirdaitė, D.; Asadauskas, S. Effects of electrolyte and Ti layers on static and dynamic friction of anodized alumina. In Proceedings of the BALTRIB'2017: Proceedings of IX International Scientific Conference: Dedicated to 100th Anniversary of Restitution of LITHUANIA, Kaunas, Lithuania, 16–17 November 2017; pp. 199–206.
18. Asadauskas, S.J.; Stalnionis, G.; Bikulcius, G.; Jankauskas, S.; Stasiunas, L.; Matijosius, T. Nanoscale deposition of Group IVB elements on anodized surfaces to reduce friction. *Mater. Today Commun.* **2021**, *29*, 103008. [[CrossRef](#)]
19. Matijošius, T.; Staišiūnas, L.; Stalnionis, G.; Asadauskas, S.J. Deposition of nanothin layers of selected elements by magnetron sputtering and ALD on anodized aluminum. In *FizTech*; Center for Physical Science and Technology: Vilnius, Lithuania, 22–23 October 2020; p. 36. [[CrossRef](#)]
20. Matijošius, T.; Staišiūnas, L.; Asadauskas, S.J. Ball-on-plate tribotesting of IVB element layers deposited on anodized aluminum alloys. *Open Access Dataset* **2021**, *1*, 1–15. [[CrossRef](#)]
21. Horváth, R.; Czifra, Á.; Drégelyi-Kiss, Á. Effect of conventional and non-conventional tool geometries to skewness and kurtosis of surface roughness in case of fine turning of aluminium alloys with diamond tools. *J. Adv. Manuf. Technol.* **2015**, *78*, 297–304. [[CrossRef](#)]
22. Wu, H.; Zhao, J.; Cheng, X.; Xia, W.; He, A.; Yun, J.H.; Huang, S.; Wang, L.; Huang, H.; Jiao, S.; et al. Friction and wear characteristics of TiO<sub>2</sub> nano-additive water-based lubricant on ferritic stainless steel. *Tribol. Int.* **2018**, *117*, 24–38. [[CrossRef](#)]
23. Padgurskas, J.; Kreivaitis, R.; Jankauskas, V.; Janulis, P.; Makarevičienė, V.; Asadauskas, S.; Miknius, L. Antiwear properties of lard methyl esters and rapeseed oil with commercial ashless additives. *Mechanics* **2008**, *70*, 67–72.
24. Iordanoff, I.; Khonsari, M.M. Granular lubrication: Toward an understanding of the transition between kinetic and quasi-fluid regime. *J. Trib.* **2004**, *126*, 137–145. [[CrossRef](#)]

**Disclaimer/Publisher's Note:** The statements, opinions and data contained in all publications are solely those of the individual author(s) and contributor(s) and not of MDPI and/or the editor(s). MDPI and/or the editor(s) disclaim responsibility for any injury to people or property resulting from any ideas, methods, instructions or products referred to in the content.